 doi:10.20944/preprints202012.0707.v1

Laser additive manufacturing of Si/ZrO_2 tunable crystalline phase 3D nanostructures†

Greta Merkininkaitė,[‡,¶] Edvinas Aleksandravičius,[§] Mangirdas Malinauskas,[§] Darius Gailevičius,[‖,¶] and Simas Šakirzanovas[*,‡,⊥]

‡*Faculty of Chemistry and Geoscience, Vilnius University,Naugarduko str. 24, Vilnius LT-03225, Lithuania*

¶*Femtika, Saulėtekio Ave. 15, Vilnius LT-10224, Lithuania*

§*Laser Research Center, Physics Faculty, Vilnius University, Saulėtekio Ave. 10, Vilnius LT-10223, Lithuania*

‖*Laser Research Center, Physics Faculty, Vilnius University Saulėtekio Ave. 10, Vilnius LT-10223, Lithuania*

⊥*Department of Chemical Engineering and Technology, Center for Physical Sciences and Technology, Saulėtekio Ave. 3, Vilnius LT-10257, Lithuania*

E-mail: simas.sakirzanovas@chf.vu.lt

Abstract

The current paper is focused on the rapidly developing field of nano-/micro three-dimensional production of inorganic materials. The fabrication method includes laser lithography of hybrid organic-inorganic materials with subsequent heat treatment leading to a variety of crystalline phases in 3D structures. In this work, it was examined a series of organometallic polymer precursors with different silicon (Si) and zirconium

†Laser additive manufacturing of Si/ZrO_2 tunable crystalline phase 3D nanostructures

Preprints (www.preprints.org) | NOT PEER-REVIEWED | Posted: 28 December 2020 doi:10.20944/preprints202012.0707.v1

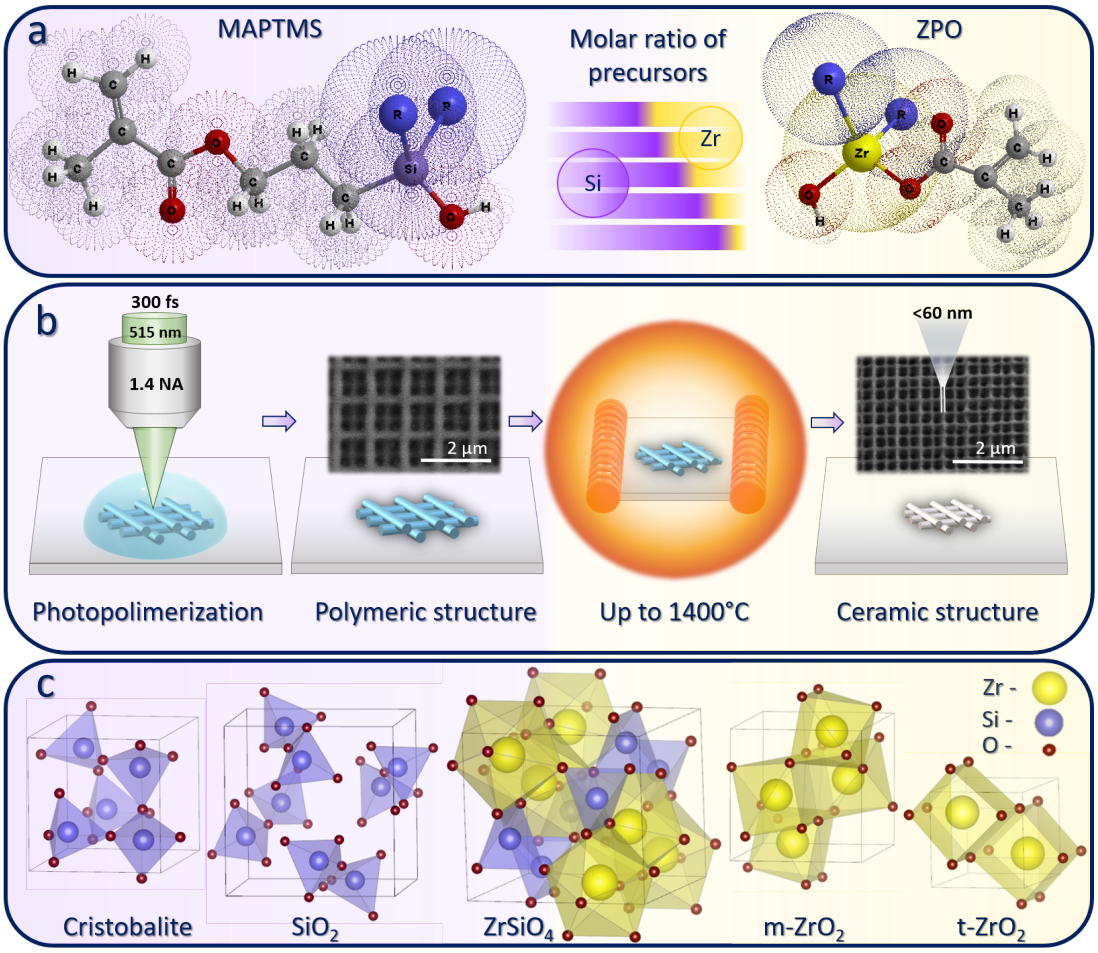

Figure 1: Graphical abstract showing precursors, their molar ratios in syntheses (a), photopolymerization and calcination technology (b) and formed crystalline phase lattices after calcination (Cristobalite, SiO_2, $ZrSiO_4$, monoclinic ZrO_2 and tetragonal ZrO_2) (c). These phases can be observed depending on the treatment temperature and initial hybrid materials compositions.

(Zr) molar ratios, ranging from 9:1 to 5:5, prepared via sol-gel method. All mixtures were examined for perspective used in 3D laser by manufacturing by fabricating nano- and micro-feature sized structures. Their deformation and surface morphology were evaluated depending on chemical composition and crystallographic phase. The appearance of a crystalline phase was proven using single-crystal X-ray diffraction analysis, which revealed a lower crystallization temperature for microstructures compared to bulk materials. Fabricated 3D objects retain a complex geometry without any distortion after heat treatment up to 1400 °C. Under the proper conditions, a zircon phase

Preprints (www.preprints.org) | NOT PEER-REVIEWED | Posted: 28 December 2020 doi:10.20944/preprints202012.0707.v1

($ZrSiO_4$ - a highly stable material) can be observed. In addition, the highest new record of achieved resolution below 60 nm has been reached. The proposed preparation protocol can be used to manufacture micro/nano-devices with high precision and resistance to high temperature and aggressive environment.

Introduction

There is no doubt that ceramics and ceramic-like materials cover an important part of science and industry, due to outstanding thermal, mechanical, chemical properties.[1] The ability to produce micro- or even nano-scale objects possessing such properties is a topic of growing attention. 3D ceramic objects can be produced using a multitude of 3D printing techniques, such as slurry-based (stereolithography, digital light processing, two-photon polymerization, injection printing, direct ink writing), powder-based (three-dimensional printing, selective laser sintering or melting), and bulk-solid based (laminated object manufacturing and fused deposition modeling).[2] Common procedures in all those listed methods are the application of ceramic particles suspension in an organic medium, which is necessary for chemical network formation. Such an approach is suitable for relatively large-scale 3D ceramic object formation, however, the main drawback of such approach is relatively low achievable resolution. One of the viable approaches to overcome this limitation is the usage of homogeneous hybrid organic-inorganic compounds for laser lithography with an additional calcination step.[3,4] The benefit of this method is the initiation of photochemical reactions with a focused light beam for 3D structuring. The homogenous organic-inorganic hybrid compound consists of two major parts: organic functional residue taking part in photopolymerization and inorganic residue leading to ceramic material after post-processing. The result of such methodology is defined as high resolution micro-and nanoscale 3D glass-ceramic crystalline objects. Up to now, a wide variety of materials such as acrylates, epoxies, hydrogels, hybrids, or biopolymers were used in a 3D laser printing.[5] It can be expected that such an abundance of tested materials will lead to nanoscale resolution of printed structures. Nanoscale features (65 $\pm$

 doi:10.20944/preprints202012.0707.v1

5 nm) have been achieved a while ago using the organic DABP-triacrylate resin.[6] However, organic materials have serious limitations regarding stability against the harsh environments. To our knowledge, the highest reported resolution for Zr-organic hybrid material is 45 nm achieved with sub-10 fs laser pulses.[7] It is worth to mention that fabricated structures are delicate in nature because even an electron microscope beam induces a serious irreversible deformation. Such mild mechanical properties can be attributed to the high content of remaining organic material.[7] Such properties bring challenges in handling and manipulating such structures. Recently, fabrication of a true-3D inorganic ceramic with an average 85 $\pm$ 10 nm line cross-section was demonstrated using a sol-gel resist precursor.[3]

Pure inorganic structures are obtained after high temperature treatment of inorganic-organic hybrid materials. After heat treatment, the derivatives shrink in size, increase in density and hardness, following with improved mechanical and chemical stability.[8,9] However, it is difficult to extract an ultra-thin line because it tends to deform or break at extremely high temperatures. Even so, it is necessary to mention, that Seniutinas et al. (2018) obtained $\approx$25 nm line width of buckyball by combining pyrolysis and oxygen plasma etching as post-processing steps.[10] Nevertheless, such a method is appropriate for obtaining simple thin structures, because it is based on the etching of the top layer of building material. This approach would be cumbersome for the production of more complex 3D or periodic bulky derivatives. Heating of hybrid materials is attractive not only because of the shrinkage in dimensions but also due to the formation of new crystalline phases expanding the application possibilities. With this in mind, the application of combined Si and Zr precursors following the thermal treatment under oxidative atmosphere open the possibility for the formation of various crystalline phases with distinctive chemical and physical properties.[11–13]

To sum up, precursors with properties required for fabrication are an essential prerequisite for 3D micro- and nano-dimension ceramic frameworks made by laser lithography. Thus, the search of new precursors suitable for laser 3D polymerization remains an urgent and timely task.

 doi:10.20944/preprints202012.0707.v1

Results and discussion

For the reasons stated above we have synthesized a few versions of the precursor SiX:ZrY, characterized it, performed 3D laser exposure and heat treatment experiments. The material is a modified silicate (ORMOSIL®) class sol-gel resist originating from SZ2080 .[14]

Beginning with the liquid and gel precursors after synthesis, the initial data from Fourier transform infrared spectroscopy (FTIR) and refractometric measurements were performed. Detailed results are shown and in the Supporting Information Fig. 1 and Fig. 2. Bond concentrations for Si-O-Zr, Zr-O-Zr, and Si-O-Zr depending on the synthesis protocol are found to be consistent. More Si results in more Si-O-Si bonds and more Zr in more Zr-O-Zr. In addition, the refractive index for each precursor is greater than 1.50 (except Si9:Zr1) which are attributed to high-refractive-index polymers (HRIP) (see supporting information Fig. 2),[15] and is also a convenient value for spherical aberration-free laser fabrication procedures and agrees with what is known from 2008 Ovsianokov et al. publication.[14] Therefore the synthesis procedure is considered valid.

Following, to explore what happens with the weight of the SiX:ZrY material during calcination, thermogravimetric analysis was performed (Fig. 2). In Fig. 2 (a) red lines show weight loss dependence on temperature, while blue lines show weight loss velocity. Firstly, the fast drop in the weight up to ≈140 °C indicating the evaporation of solvents. According to FTIR spectra (see supporting information Fig. 1 (c)) was found that materials could be almost thermally polymerized at 140 °C temperature. Therefore, weight loss was calculated for the phase transition from the polymeric (140-150 °C) to the inorganic (600-700 °C) material. Undoubtedly, during these periods the organic component of the hybrid materials is decomposed. Furthermore, at this stage several changes in weight loss are observed, indicating that different organometallic components decompose at different temperatures.

Preprints (www.preprints.org) | NOT PEER-REVIEWED | Posted: 28 December 2020 doi:10.20944/preprints202012.0707.v1

Moreover, it was established that with increasing silicon content, weight loss increases and it ranges from 51% to 62% (Fig. 2 (b (black))). It is necessary to mention, that with a higher amount of zirconium, the pure inorganic material is achieved at lower temperatures. Along with weight loss, the volume also shrinks (Fig. 2 (b (red), c and d). The change in volume after heating was estimated from the change in volume of fabricated cubes (three cubes were fabricated with each material (the results are presented in a supporting information table 1. The volume changes exceeded all weight changes. This indicates that the obtained inorganic structure is denser compared to the original polymeric structure. It also can be concluded that denser ceramic structures are obtained by increasing the zirconium content, because the weight loss line direction coefficient is higher (Fig. 2 (b (black)) compared to the volumetric shrinkage line direction coefficient (Fig. 2 (b (red)) in the range from Si9:Zr1 to Si5:Zr5.

To clarify the fabrication prospects of proposed mixtures, woodpiles were fabricated (Fig. 3). It was found that the highest resolution of the inorganic structure (58.7 $\pm$ 1.5 nm) is achieved for Si9:Zr1 material using 64 μW power and 200 μm/s velocity followed by annealing at 1000 °C (Fig. 3f). The higher power was not used due to uncontrolled burning of Si9:Zr1 material at 300 fs, 515 nm pulses, and 1.4 NA objective conditions. To the best of our knowledge this is the highest resolution for inorganic 3D ceramic derivative achieved by printing up to this day. The same woodpiles were fabricated with all hybrids for resolution comparison of all materials. The dependence of woodpile lines width on the laser energy density is shown in figure 3 g, f and the numerical values are listed in supporting information tables 2, 3, 4, and 5. At lower energy densities it is difficult to get a clear relationship between resolution and material composition, nevertheless, at higher laser energy densities (from 24 $\mu J/\mu m^3$ to 32 $\mu J/\mu m^3$) it is evident that the resolution is higher where the zirconium content is lower. In prepared mixtures, the zirconium amount is linked to the methacrylic acid, while the silicon amount corresponds to the methyl methacrylate functional group. The resolution dependence of 3D derivatives changing composition can be explained by the fact that the photopolymerization activation energy of methacrylic acid is several times lower than the

Preprints (www.preprints.org) | NOT PEER-REVIEWED | Posted: 28 December 2020 doi:10.20944/preprints202012.0707.v1

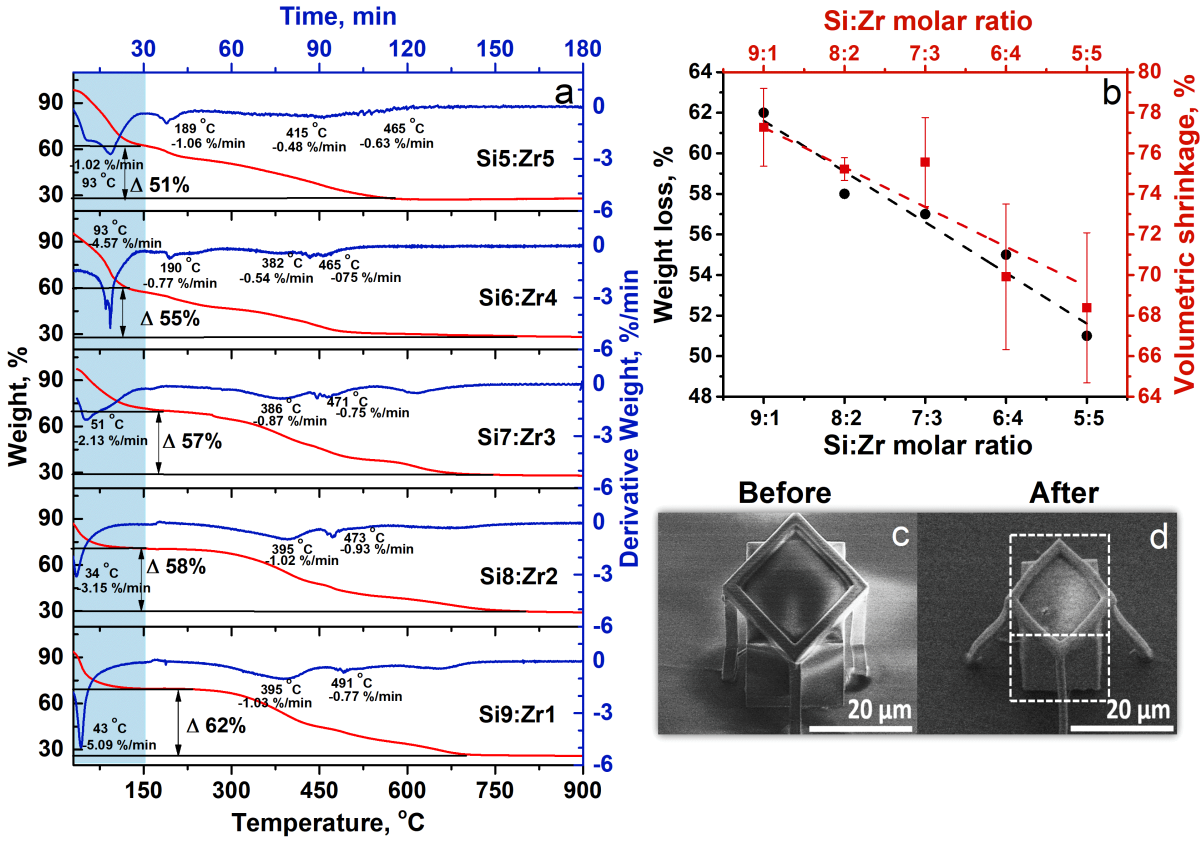

Figure 2: TGA data of SiX:ZrY showing weight loss vs. temperature (red line) and weight loss velocity (blue line) (a), weight loss for the phase transition from the polymeric to the glass/ceramic phase (black) and volumetric shrinkage of cubes at the same phase transition (red) (b), c and d show SEM images of the Si7:Zr3 cube before and after heat treatment at 1000 °C.

activation energy of the methyl methacrylate under the same conditions (E_a(methacrylic acid)=1.79 kcal/mol, E_a(methyl methacrylate)=4.48 kcal/mol).[16] The same laser energy density tends to polymerize a larger volume of material with a lower photopolymerization activation energy during the unit pulse. However, photopolymerization activation energy may also depend on the influence of adjacent functional groups, photoinitiators, quenchers, and/or ambient conditions.[17] The printed structure treatment in a developing solvent after photopolymerization can also affect the resolution due to the solvent ability to dissolve the unpolymerized monomer molecules at the phase junction between polymer and gel. The higher solvent affinity to substance and the lower molecular weight or less branched

 doi:10.20944/preprints202012.0707.v1

structure of the molecule (steric effect), the better solubility is achieved. The molecular weight and branching are smaller for zirconium and methacrylic acid monomer compared to silicon monomer. Accordingly, as the zirconium content increases, the resolution of the 3D structure should increase too, different from the reaction activation energy influence. The competition takes place between two opposing processes. This fact explains why it is difficult to see the evident dependence of the resolution on the composition of the material at low laser energy densities. Similarly, the easier penetration of the solvent into the material can affect the swelling of the polymeric structure. It is important to mention that the solubility of materials depends on many factors, thus it is used here only for a comparison.

In Fig. 4, Fig. 5 and Fig. 6 XRD data of scaffolds (a-e) and corresponding powders (g-l) are presented for samples annealed at 1000 °C, 1200 °C and 1400 °C, respectively. At the lowest annealing temperature (Fig. 4) in both, scaffolds and powders, the formation of crystalline cristobalite and tetragonal ZrO_2 phases are observed. Increasing zirconium amount leads to a more pronounced tetragonal ZrO_2 crystalline phase. However, a relatively high background in diffractograms indicates the presence of an amorphous phase. No visible deformations in 3D structures were observed for all series of samples with different compositions after calcination at 1000 °C. With increasing annealing temperature to 1200 °C (Fig. 5) leads to samples, both powder, and structures, with higher crystallinity. However, X-ray diffraction data for all samples still provide evidence of glassy amorphous phase presence. Diffractogram of Si5:Zr5 3D structure shows that the cristobalite phase remains as pronounced as tetragonal ZrO_2, while different behavior is observed for powder sample, tetragonal ZrO_2 phase is dominating. Each 3D structure preserves its shape after 1200 °C heat treatment, except Si9:Zr1. The materials with the higher initial amount of silicon, start to melt due to the lower melting temperature of silicon oxide compared to zirconium oxides. The most stable zirconium dioxide phase is monoclinic, while tetragonal and cubic phases tend to form at higher temperatures.[18] However, in our study, the monoclinic ZrO_2 phase formed only at 1400 °C (see Fig. 6a-g), while tetragonal dominated at all annealing temperatures and starting

Preprints (www.preprints.org) | NOT PEER-REVIEWED | Posted: 28 December 2020 doi:10.20944/preprints202012.0707.v1

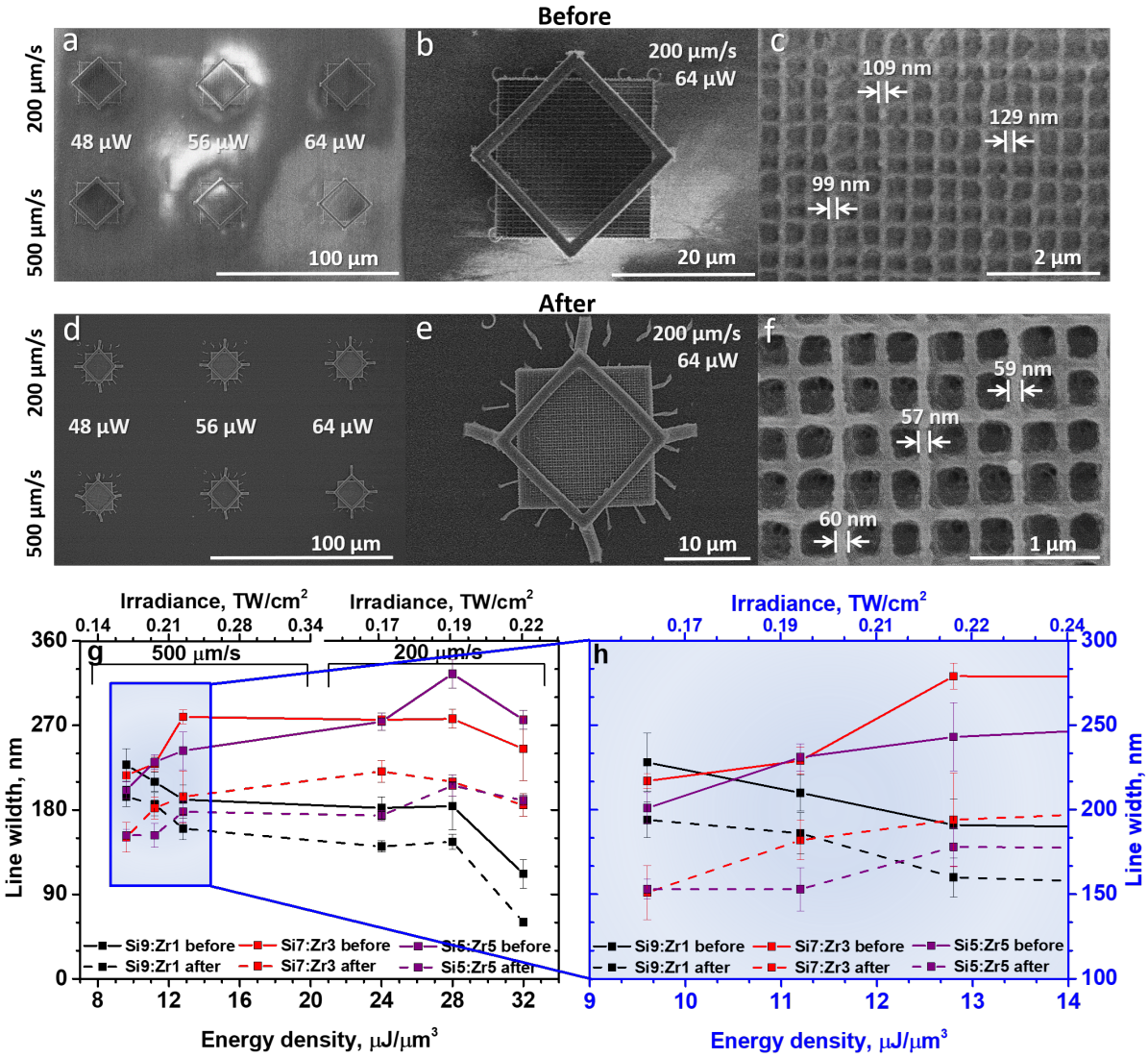

Figure 3: Si9:Zr1 woodpiles before heat treatment (a, b, c) and after heating at 1000 °C under air atmosphere (d, e, f). a,d- on the top line- woodpiles fabricated at 200 μm/s speed and 48, 56, 64 μW power, respectively, while on the bottom line- woodpiles fabricated at 500 μm/s speed and 48, 56, 64 μW incident irradiation power, respectively. b, c, e, and d photonic crystal fabricated at 200 μm/s and 64 μW with the highest obtained resolution. g- the dependence of Si9:Zr1, Si7:Zr3, Si5:Zr5 woodpiles lines width on the laser energy density. Before heat treatment- solid lines, after- dashed lines. h- zoomed part of g graph. Catastrophic breakdown of Si9:Zr1 occurs with more than 32 $\mu J/\mu m^3$.

compositions (except Fig. 6g). Such phenomenon can be explained using Ostwald's Step Rule, stating that phase formation follow a general pattern when phases with the highest energy are formed first following the transition to lower energy phases.[19,20] This means that

Preprints (www.preprints.org) | NOT PEER-REVIEWED | Posted: 28 December 2020 doi:10.20944/preprints202012.0707.v1

the higher energy metastable tetragonal phase is frozen in prepared samples. Recently, A. Auxéméry et al. demonstrated that it is possible to stabilize metastable tetragonal ZrO_2 not only by cationic substitution but it can be achieved by varying the synthesis conditions.[21]

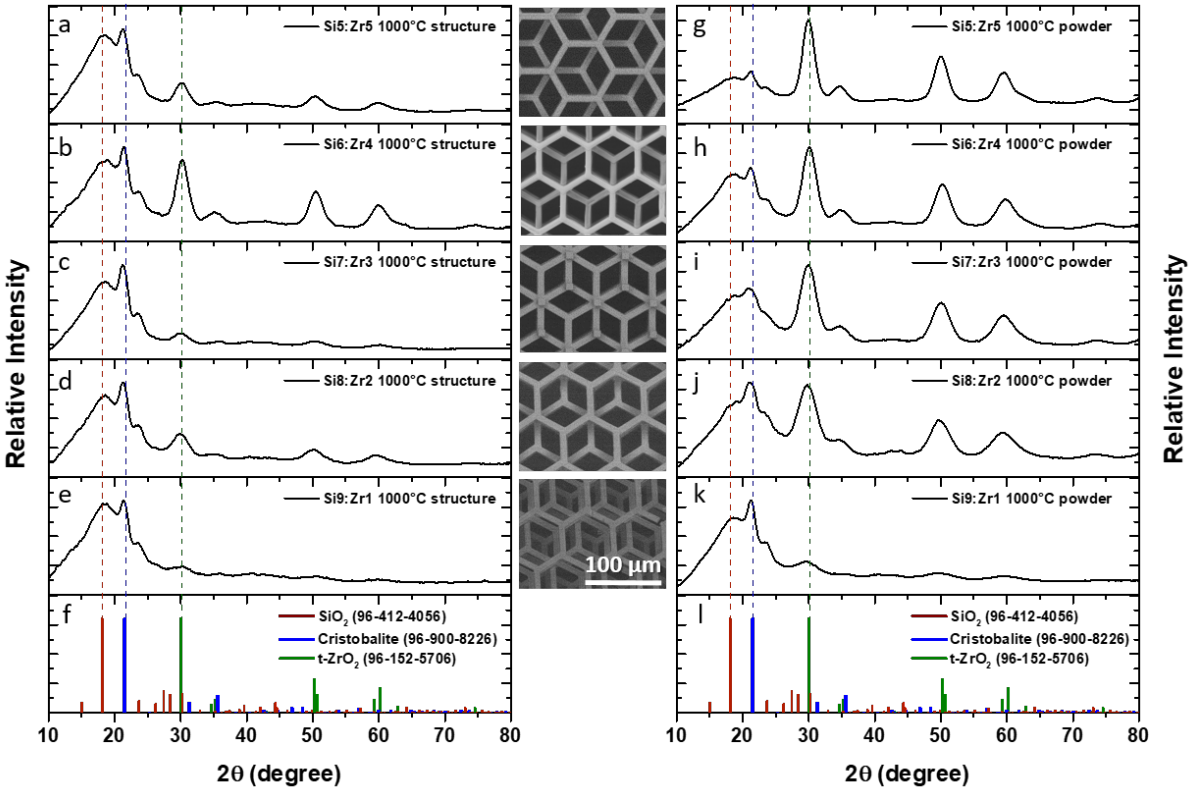

Figure 4: X-ray diffractograms of structures (SEM images) annealed at 1000 °C (a-Si5:Zr5, b-Si6:Zr4, c-Si7:Zr3, d-Si8:Zr2, e-Si9:Zr1, f-reference data) and X-ray diffractograms of powders annealed at 1000 °C (g-Si5:Zr5, h-Si6:Zr4, i-Si7:Zr3, j-Si8:Zr2, k-Si9:Zr1, l-reference data). SEM images show corresponding 3D scaffolds treated at 1000 °C temperature. SEM images correspond to the same scale bar.

Moreover, the resistance of ceramic structures to aggressive chemicals has also been investigated and the results are depicted in the supporting information Fig.3. This study confirmed that ceramic structures have a higher resistance to chemicals compared to the corresponding polymeric.

Currently, thermal post-treatment is being established as a technique for downscaling or improving the properties of the laser additively manufactured 3D nanostructures. For instance, it was reported to apply pyrolysis at 900 °C for production of carbon nanowires,

Preprints (www.preprints.org) | NOT PEER-REVIEWED | Posted: 28 December 2020 doi:10.20944/preprints202012.0707.v1

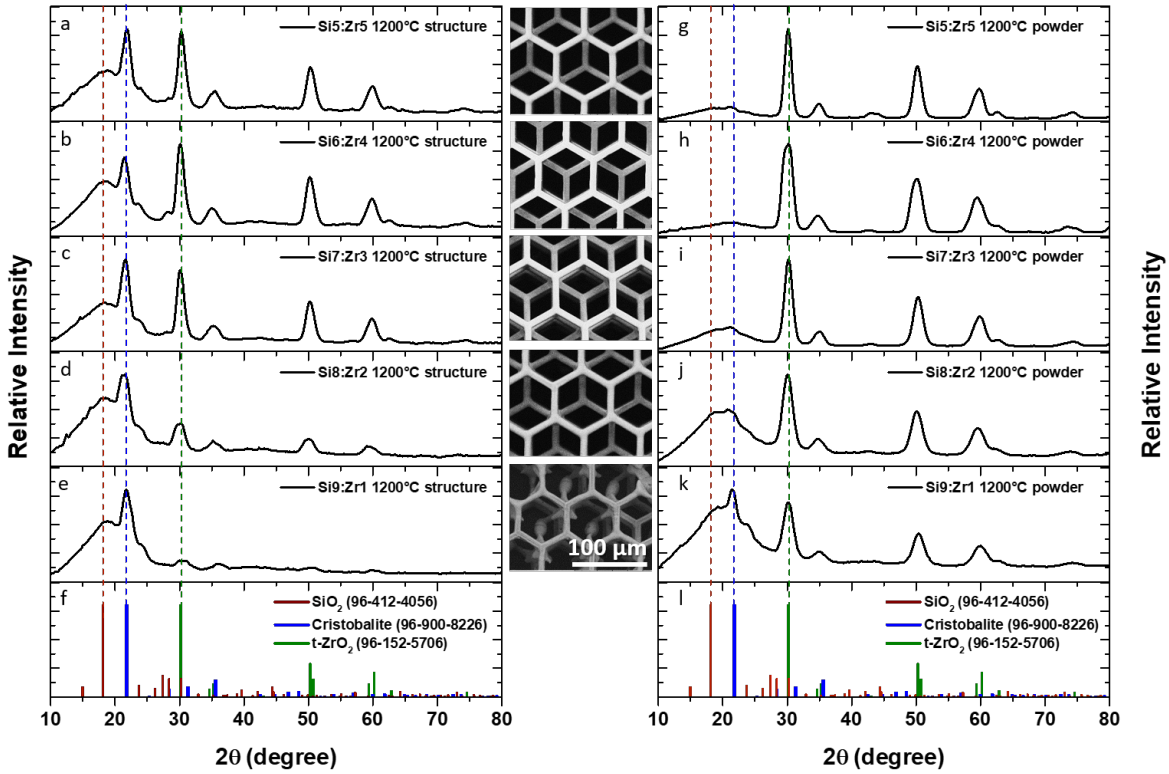

Figure 5: X-ray diffractograms of structures (SEM images) annealed at 1200 °C (a-Si5:Zr5, b-Si6:Zr4, c-Si7:Zr3, d-Si8:Zr2, e-Si9:Zr1, f-reference data) and X-ray diffractograms of powders annealed at 1200 °C (g-Si5:Zr5, h-Si6:Zr4, i-Si7:Zr3, j-Si8:Zr2, k-Si9:Zr1, l-reference data). SEM images show corresponding 3D scaffolds treated at 1200 °C temperature. SEM images correspond to the same scale bar.

which was successful for both downscaling the features and converting the compound into a new substance.[22]

However, the resulting material made of purely organic resin was still an organic one, though with significantly improved properties such as high isotropy, electrochemical stability, biocompatibility, chemical resistance, and semiconductor-like electrical parameters, making it attractive for manufacturing Carbon-MEMS.

In parallel, a single crack-free pre-ceramic resin for two-photon lithography was developed and studied for making bulky and free-form structures,[23] yet the systematic feature size (resolution) study was not performed in details, making the findings difficult to evaluate or compare in between.

Preprints (www.preprints.org) | NOT PEER-REVIEWED | Posted: 28 December 2020 doi:10.20944/preprints202012.0707.v1

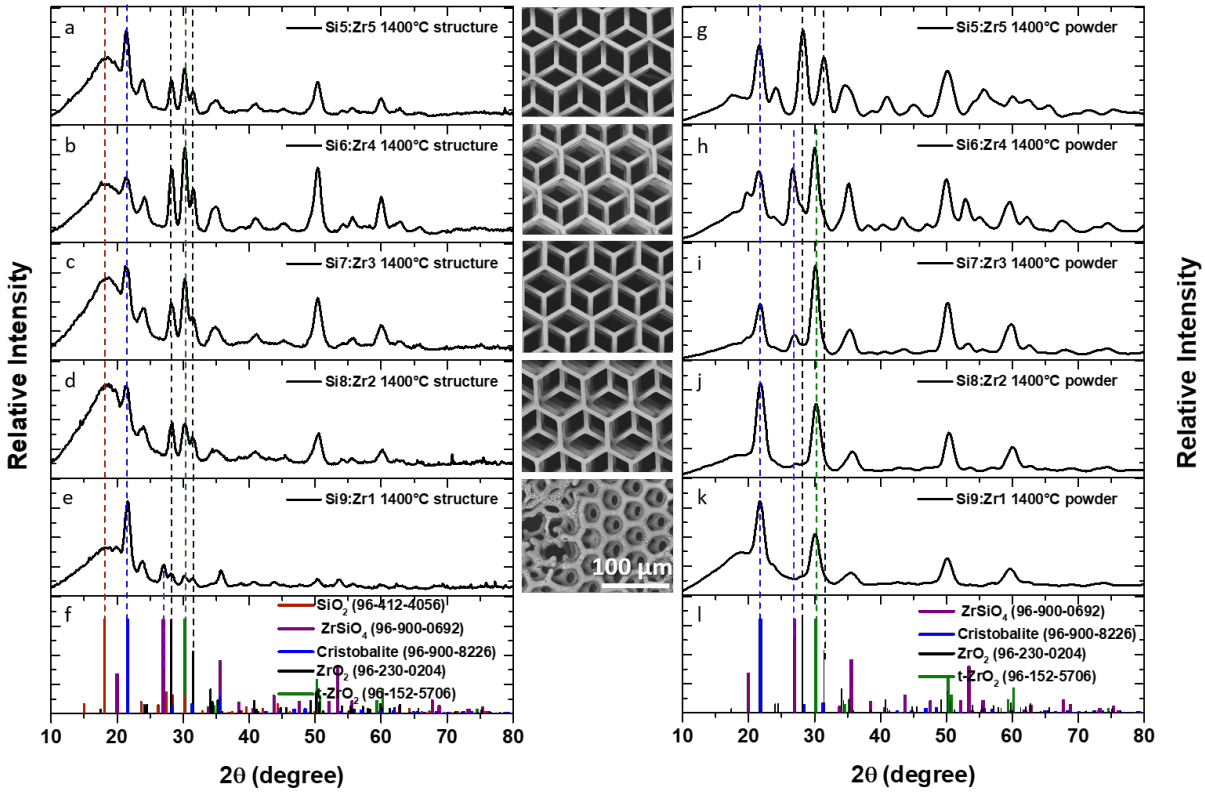

Figure 6: X-ray diffractograms of structures (SEM images) annealed at 1400 °C (a-Si5:Zr5, b-Si6:Zr4, c-Si7:Zr3, d-Si8:Zr2, e-Si9:Zr1, f-reference data) and X-ray diffractograms of powders annealed at 1400 °C (g-Si5:Zr5, h-Si6:Zr4, i-Si7:Zr3, j-Si8:Zr2, k-Si9:Zr1, l-reference data). SEM images show corresponding 3D scaffolds treated at 1400 °C temperature. SEM images correspond to the same scale bar.

On the other hand, some inorganic tin oxide ceramics were 3D structured via a similar femtosecond laser 3D photolithography technique followed by sintering, it showed a promising route for high definition additive manufacturing. Yet the obtained spatial resolution was ≈1 μm in linewidth,[24] thus roughly one order less in respect to the values achieved here. Up to date, the highest reported feature size was ≈200 nm and the used material was SiOC ceramics,[25] but without the phase tunability or possibility to achieve crystalline material.

The latest research towards applications in photonics was focused on creating high refractive index materials, such as TiO_2, again the spatial resolution within the range 300 – 600 nm.[26] All in all, the results achieved in this study are ground braking in the context of repeatable additive manufacturing accuracy and crystalline phase tunability of 3D

Preprints (www.preprints.org) | NOT PEER-REVIEWED | Posted: 28 December 2020 doi:10.20944/preprints202012.0707.v1

nanostructures.

Conclusions

It is shown that the hybrid organic-inorganic polymer resists of variable composition SiX:ZrY can be directly 3D laser structured and heat-treated to produce micro- and nanostructures of different SiO_2/ZrO_2 inorganic phases. In particular, along with a typical amorphous (glass), t-ZrO_2 and monoclinic cristobalite, the new m-ZrO_2 and zircon phases have been detected.

The t-ZrO_2 and cristobalite phases are observed after calcination at 1000 to 1400 °C for all initial compositions Si5:Zr5-Si9:Zr1. However, the m-ZrO_2 and zircon polycrystalline phases are mostly pronounced in printed Si6:Zr4 and Si9:Zr1 composition samples after treatment at 1400 °C. This procedure is essential and relevant at the micro/nano-scale leading to individual feature size below 100 nm, while 3D additive manufacturing methods of hard inorganic materials is far from being readily available.

Repeatable nanoscale features size down to 60 nm were achieved for the composition of Si9:Zr1 heat-treated at 1000 °C. The resolution is proven for fine woodpile geometry periodic 3D structures. This is the highest resolution achieved for an ORMOSIL® class material using laser additive manufacturing based on multi-photon lithography and thermal post-processing.

In perspective, further variation in composition of the metalorganic prepolymer SiX:ZrY in finer steps could yield more fine-adjusted physical and chemical properties. This should be expected not only for the examined current composition, but for other multicomponent metalorganic polymer mixtures. Such approach is highly promising, especially with combination with localised annealing methods, e.g. focused electron or ion beam, as well as a focused infrared laser radiation could generate a 3D structures with varying and controllable material properties throughout all 3D structure. Besides, proposed preparation approach is promising for 4D printing of inorganic smart/programmable materials.

Preprints (www.preprints.org) | NOT PEER-REVIEWED | Posted: 28 December 2020 doi:10.20944/preprints202012.0707.v1

Experimental

Materials and Synthesis

Photoactive preceramic polymers were synthesized by the sol-gel method according to the synthesis described in Ovsianikov et. al. article (2008).[14] 3-(Trimethoxysilyl)propyl methacrylate (MAPTMS, Sigma Aldrich, 98%), zirconium(IV) propoxide solution 70 wt. % in 1-propanol (ZPO, Sigma Aldrich) and 2-methacrylic acid contains 250 ppm MEHQ as inhibitor (MAA, Sigma Aldrich, 99%) were selected as precursors for the preparation of the preceramic photopolymer. Methacrylic acid was distilled in a vacuum in order to remove the inhibitor. Other reagents were used without further purification. First of all, MAPTMS was hydrolyzed using aqueous HCl (0.1 M) solution at a 1:1 molar ratio. After a half of hour of stirring the solution of alkoxysilane and water becomes homogeneous, which means that hydrolysis of the alkoxysilane groups has occurred.

Simultaneously, ZPO was stabilized by MAA at a 1:1 molar ratio. After that, hydrolyzed MAPTMS was added dropwise to the stabilized ZPO solution to form a liquid sol. The photoinitiator was not used. After stirring for 12 h in a sealed vial, the material was filtered using a 0.22 μm syringe filter. One series (5 compounds) of SiX:ZrY metalorganic compound was synthesized, where X is Si molar ratio from 9 to 5 and Y is Zr molar ratio from 1 to 5, respectively. Five samples were prepared by sols drops adding on substrates, and the drops were dried on a hotplate at 90 °C degree for 1 hour in order to form monomers with inorganic condensation links causing to make gels.

For the chemical resistance investigation, a mixture of concentrated sulfuric acid (Chempur, 95-98%) and peroxide (Chempur, 50%) in a volume ratio of 4:1, respectively, (known as piranha) was used.

Preprints (www.preprints.org) | NOT PEER-REVIEWED | Posted: 28 December 2020 doi:10.20944/preprints202012.0707.v1

3D lithography and heat treatment

Structure fabrication was carried out by direct laser writing, using 300 fs 515 nm pulses at a frequency of 200 kHz.[4] During woodpiles fabrication average laser power was 48, 56, and 64 μW, focused with a 100x1.4 NA objective, beam scanning speed was 200 and 500 μm/s, hatching distances in both, x and y axes, was 0.1 μm. Fabrication of scaffolds was done with an average laser power of 655 μW, focused with a 20x0.8 NA objective. The energy density was calculated employing the following equation:

$$E_{ACC} = \frac{P}{v\Delta h_x \Delta h_y}, \tag{1}$$

where E_{ACC}- laser volumetric energy density [μJ/μm^3], P- average laser power [μW], v- scanning speed [μm/s], Δh_x and Δh_y [μm]- hatching distances in x and y axis, respectively.

To be comparable with more frequently used parameter we also calculated the irradiance for each case applying the following formula:[27]

$$I = \frac{E_p}{\tau_p \pi \omega^2}, \tag{2}$$

here I is irradiance [TW/cm^2], E_p=P/f, where P [mW] is average laser power, f- repetition rates [kHz], τ_p is the pulse duration [fs], $\omega = 0.61\lambda/\mathrm{NA}$ [nm].

In order to remove the organic part from the fabricated organometallic structures and form an inorganic, glassy, or ceramic/crystalline, structures were heated at a high temperature. Cubes and woodpiles were annealed on corundum substrates for 1 h at 1000 °C, under air atmosphere, the rate of temperature rise was 5 °C/min. While scaffolds were annealed on graphite substrates at 1000 °C, 1200 °C, 1400 °C, under air atmosphere, the rate of temperature rise was also 5 °C/min.

Preprints (www.preprints.org) | NOT PEER-REVIEWED | Posted: 28 December 2020 doi:10.20944/preprints202012.0707.v1

Measurements

The X-ray diffraction data of SiX:ZrY 3D structures and powders annealed at 1000 °C, 1200 °C and 1400 °C were collected on a BRUKER AXS (D8 Quest System) X-ray diffractometer equipped with PHOTON 100 CMOS detector. The X-ray generator was operated at 50 kV and 20 mA using Mo Kα (λ = 0.71073 Å) radiation. Annealed 3D micro-structures and powders were placed on the measuring needle (Fig. 7 (d)), obtained X-ray diffraction data (Debye-Scherrer rings (Fig. 7 (c)) were collected and integrated using Bruker Apex 3 software. Obtained X-ray diffractograms were recalculated to Cu Kα (λ = 1.541874 Å) wavelength using Bragg's law and data were compared to the reference data (Fig. 7 (a, b)).

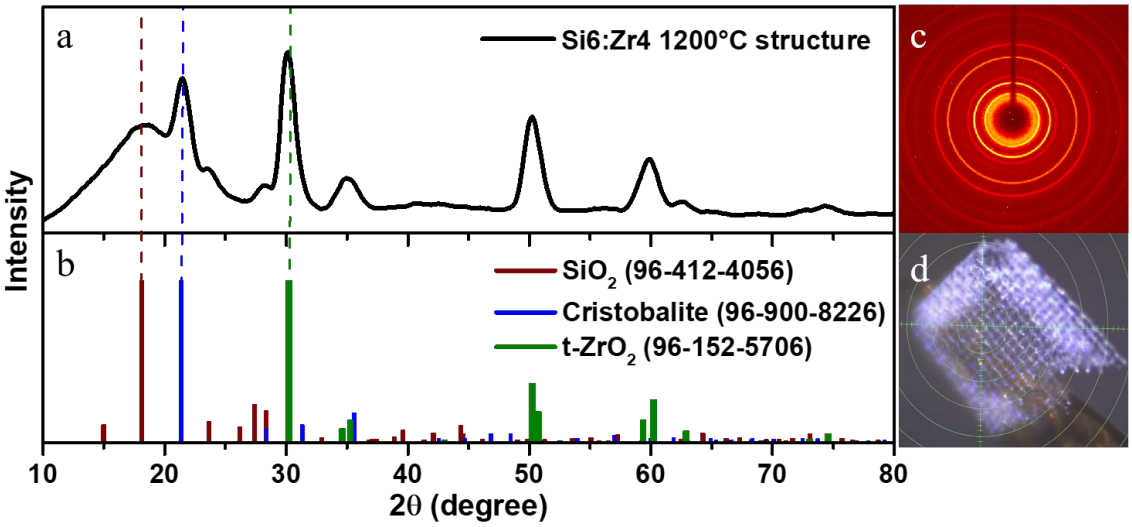

Figure 7: X-ray diffraction measurements. a- X-Ray diffraction pattern of Si6:Zr4 structure annealed at 1200 °C temperature, b- reference patterns, c- Debye-Scherrer rings obtained after X-Ray diffraction measurement, d- photograph of Si6:Zr4 structure annealed at 1200 °C temperature before measurement.

Fourier transform infrared spectroscopy (FTIR) spectra of SiX:ZrY sols, gels, and polymer powders (thermally polymerized at 140 °C) were recorded in transmission mode using FTIR spectrometer ALPHA (Bruker, Inc.), equipped with a room temperature detector DLATGS. Spectra were acquired from 100 interferogram scans with 2 cm^{-1} resolution, from 4000 to 485 cm^{-1} wavenumbers.

For thermogravimetric (TGA) analysis, Pyris 1 TGA (Perkin Elmer) equipment was used; all SiX:ZrY sols were heated under air atmosphere from 30 °C to 900 °C with a heating rate of 5 °C/min.

Refractive indices of sols and gels were collected using Abbemat MW Multiwavelengths Refractometer with YAG (Yttrium-Aluminium-Garnet) prism, white light LED source, and 6 filters at different wavelengths: 436.5, 486, 513.5, 546.3, 589.3, 643.3 nm. Measurements were performed at 25 °C temperature.

The SEM images of woodpiles and cubes before and after heat treatment were taken with a FE-SEM Hitachi SU-70. The SEM images together with EDS of scaffolds were taken with a lower resolution scanning electron microscope- Hitachi TM3000. The elemental analysis was carried out with 15 kV accelerating voltage.

Acknowledgement

The US AMRDEC grant No. W911NF-16-2-0069 "*Enhanced Absorption in Stopped-Light Photonic Nanostructures: Applications to Efficient Sensing*" and EU LASERLAB-EUROPE (grant agreement No. 871124, Horizon 2020 research and innovation programme) projects are acknowleged for the financial support.

In addition, authors are grateful to Rokas Vargalis for taking high resolution SEM images.

 doi:10.20944/preprints202012.0707.v1

References

(1) Janssen, R.; Scheppokat, S.; Claussen, N. Tailor-made ceramic-based components—Advantages by reactive processing and advanced shaping techniques. *J. Eur. Ceram. Soc.* **2008**, *28*, 1369 – 1379.

(2) Chen, Z.; Li, Z.; Li, J.; Liu, C.; Lao, C.; Fu, Y.; Liu, C.; Li, Y.; Wang, P.; He, Y. 3D printing of ceramics: A review. *J. Eur. Ceram. Soc.* **2019**, *39*, 661 – 687.

(3) Gailevičius, D.; Padolskytė, V.; Mikoliūnaitė, L.; Šakirzanovas, S.; Juodkazis, S.; Malinauskas, M. Additive-manufacturing of 3D glass-ceramics down to nanoscale resolution. *Nanoscale Horiz.* **2019**, *4*, 647–651.

(4) Jonušauskas, L.; Gailevicius, D.; Mikoliunaite, L.; Sakalauskas, D.; Sakirzanovas, S.; Juodkazis, S.; Malinauskas, M. Optically Clear and Resilient Free-Form μ-Optics 3D-Printed via Ultrafast Laser Lithography. *Materials* **2017**, *10*, 12.

(5) Jonusauskas, L.; and. M. Malinauskas, S. J. Optical 3D printing: bridging the gaps in the mesoscale. *J. Opt.* **2018**, *20*, 053001.

(6) Haske, W.; Chen, V.; Hales, J.; Dong, W.; Barlow, S.; Marder, S.; Perry, J. 65 nm feature sizes using visible wavelength 3-D multiphoton lithography. *Opt. Express* **2007**, *15*, 3426–3436.

(7) Emons, M.; Obata, K.; Binhammer, T.; Ovsianikov, A.; Chichkov, B.; Morgner, U. Two-photon polymerization technique with sub-50 nm resolution by sub-10 fs laser pulses. *Opt. Mater. Express* **2012**, *2*, 942–947.

(8) Bauer, J.; Schroer, A.; Schwaiger, R.; Kraft, O. Approaching theoretical strength in glassy carbon nanolattices. *Nat. Mater.* **2016**, *15*, 438–443.

(9) Zhang, X.; Vyatskikh, A.; Gao, H.; Greer, J. R.; Li, X. Lightweight, flaw-tolerant, and ultrastrong nanoarchitected carbon. *Proc. Nat. Acad. Sci.* **2019**, *116*, 6665–6672.

(10) Seniutinas, G.; Weber, A.; Padeste, C.; Sakellari, I.; Farsari, M.; David, C. Beyond 100 nm resolution in 3D laser lithography — Post processing solutions. *Microelectron. Eng.* **2018**, *191*, 25 – 31.

(11) Kaiser, A.; Lobert, M.; Telle, R. Thermal stability of zircon ($ZrSiO_4$). *J. Eur. Ceram. Soc.* **2008**, *28*, 2199 – 2211.

(12) Nakamori, F.; Ohishi, Y.; Muta, H.; Kurosaki, K.; Fukumoto, K.; Yamanaka, S. Mechanical and thermal properties of $ZrSiO_4$. *J. Nucl. Sci. Technol.* **2017**, *54*, 1267–1273.

(13) Chiker, F.; Boukabrine, F.; Khachai, H.; Khenata, R.; Mathieu, C.; Binomran, S.; Syrotyuk, S.; Ahmed, W.; Murtaza, G. Investigating the Structural, Thermal, and Electronic Properties of the Zircon-Type $ZrSiO_4$, $ZrGeO_4$ and $HfSiO_4$ Compounds. *J. Electron. Mater.* **2016**, *45*.

(14) Ovsianikov, A.; Viertl, J.; Chichkov, B.; Oubaha, M.; MacCraith, B.; Sakellari, I.; Giakoumaki, A.; Gray, D.; Vamvakaki, M.; Farsari, M.; Fotakis, C. Ultra-Low Shrinkage Hybrid Photosensitive Material for Two-Photon Polymerization Microfabrication. *ACS Nano* **2008**, *2*, 2257–2262.

(15) Liu, J.; Ueda, M. High refractive index polymers: fundamental research and practical applications. *J. Mater. Chem.* **2009**, *19*, 8907–8919.

(16) Zhou, Q. L. T. Y. G. C. J. E. S., H. Li; Hoyle, C. E. Photopolymerization of Acid Containing Monomers: Real-Time Monitoring of Polymerization Rates. *Macromolecules* **2006**, *39*, 8269–8273.

(17) Sakellari, I.; Kabouraki, E.; Gray, D.; Purlys, V.; Fotakis, C.; Pikulin, A.; Bityurin, N.; Vamvakaki, M.; Farsari, M. Diffusion-Assisted High-Resolution Direct Femtosecond Laser Writing. *ACS Nano* **2012**, *6*, 2302–11.

(18) Liu, L.; Ma, Z.; Yan, Z.; Zhu, S.; Gao, L. The ZrO_2 formation in ZrB_2/SiC composite irradiated by laser. *Materials* **2015**, *8*, 8745–8750.

(19) Van Santen, R. A. The Ostwald step rule. *J. Phys. Chem.* **1984**, *88*, 5768–5769.

(20) Threlfall, T. Structural and Thermodynamic Explanations of Ostwald's Rule. *Org. Proc. Res. & Develop.* **2003**, *7*, 1017–1027.

(21) Auxéméry, A.; Philippot, G.; Suchomel, M. R.; Testemale, D.; Aymonier, C. Stabilization of Tetragonal Zirconia Nanocrystallites Using an Original Supercritical-Based Synthesis Route. *Chem. Mater.* **2020**, *32*, 8169–8181.

(22) Cardenas-Benitez, B.; Eschenbaum, C.; Mager, D.; Korvink, J.; Madou, M.; Lemmer, U.; De Leon, I.; Martinez-Chapa, S. Pyrolysis-induced shrinking of three-dimensional structures fabricated by two-photon polymerization: experiment and theoretical model. *Microsyst. Nanoeng.* **2019**, *5*, 38.

(23) Konstantinou, G.; Kakkava, E.; Hageluken, L.; Sasikumar, P.; Wanga, J.; Makowska, M.; Blugan, G.; Nianias, N.; Marone, F.; Van Swygenhoven, H.; Brugger, J.; Psaltis, D.; Moser, C. Additive micro-manufacturing of crack-free PDCs by two-photon polymerization of a single, low-shrinkage preceramic resin. *Add. Manuf.* **2020**, *35*, 101343.

(24) Chai, N.; Liu, Y.; Yue, Y.; Wei, P.; Wang, X.; Zhao, J.; Zhang, Q.; Huang, F.; Zeng, Z.; Gan, Z.; Mai, L.; Cheng, Y. Tin Oxide Ceramics 3D Nonlinear Photolithography via Femtosecond Laser. *Sci. Chi. Mater.* **2020**, *in press*, 00.

(25) Bauer, J.; Crook, C.; Izard, A.; Eckel, Z.; Ruvalcaba, N.; Schaedler, T.; Valdevit, L. Additive Manufacturing of Ductile, Ultrastrong Polymer-Derived Nanoceramics. *Matter* **2019**, *1*, 1–10.

 doi:10.20944/preprints202012.0707.v1

(26) Vyatskikh, A.; Ng, R.; Edwards, B.; Briggs, R.; Greer, J. Additive Manufacturing of High-Refractive-Index, Nanoarchitected Titanium Dioxide for 3D Dielectric Photonic Crystals. *Nano Lett.* **2020**, *20*, 3513–3520.

(27) Malinauskas, M.; Danilevičius, P.; Juodkazis, S. Three-dimensional micro-/nano-structuring via direct write polymerization with picosecond laser pulses. *Opt. Express* **2011**, *19*, 5602–5610.